The Bioscan AN INTERNATIONAL QUARTERLY JOURNAL OF LIFE SCIENCES 21(3): 420-435, 2026 www.thebioscan.com

Integrated Network Pharmacology, In Vitro Validation, and Molecular Simulation Approaches Reveal the Neuroprotective Mechanisms of *Colocasia esculenta* Against Alzheimer's Disease

Sakshi Huliyar[1], Nayeem Khatib[1*], Vishal S Patil[1], Sunny Gupta[1], Sonali Kuppast[1]

[1]Department of Pharmacology and Toxicology KLE College of Pharmacy, Airport Road, Basvana Kudachi. Belagavi-591124, KLE Academy of Higher education and Research (KAHER) Belagavi, 590010, Karnataka, India.

Corresponding Author: Dr. Nayeem Khatib, nakhatib@klepharm.edu, ORCID ID-0000-0001-5284-2363

DOI: https://doi.org/10.63001/tbs.2026.v21.i03.pp420-435

KEYWORDS
***Colocasia esculenta*, Alzheimer's disease, *Insilico* studies, CHRM1, ACHE, Molecular docking.**

Received on: 24/06/2026

Revised on: 01/07/2026

Accepted on: 07/07/2026

Published on: 15/07/2026

Abstract

This study evaluated the antioxidant, anti-cholinesterase, and neuroprotective potential of the ethanolic leaf extract of Colocasia esculenta using in vitro and in silico approaches against Alzheimer's disease (AD). The extract exhibited significant antioxidant activity in DPPH and FRAP assays with IC_{50} values of 51.49 µg/mL and 47.55 µg/mL, respectively, along with notable acetylcholinesterase inhibitory activity (IC_{50} = 85.24 µg/mL). LC-MS analysis identified major bioactive compounds including pelargonidin-3-glucoside and luteolin 7-O-glucoside. Network pharmacology revealed key AD-related targets such as CHRM1, ACHE, GSK3B, DRD2, and GRIN1, with involvement of PI3K-Akt, calcium, TNF, and IL-17 signaling pathways. Molecular docking demonstrated strong binding interactions of the identified phytoconstituents with ACHE and CHRM1 proteins, while molecular dynamics simulation confirmed the stability of the ligand-protein complexes. Overall, the findings suggest that Colocasia esculenta possesses promising multi-target neuroprotective activity and may serve as a potential natural candidate for Alzheimer's disease management.

1. INTRODUCTION

Alzheimer's disease (AD) is the most common cause of dementia, particularly affecting individuals aged 65 years and above, and represents a major global health concern (1) Zhang XX, et.al., (2021). Dementia is a clinical condition characterized by a progressive decline in memory, language, problem-solving ability, and other cognitive functions that significantly interfere with daily life (2) Duan Y, et.al., (2021). AD, as a chronic and progressive neurodegenerative disorder, leads to a gradual deterioration in cognitive domains such as memory, orientation, judgment, and reasoning. The prevalence of this age-related disorder is increasing rapidly, with projections indicating that approximately one in 85 individuals worldwide may be affected by AD by the year 2050 (3) Safiri S, et.al., (2024). The key pathological features of Alzheimer's disease are characterized by the deposition of extracellular beta-amyloid plaques along with the formation of intracellular neurofibrillary tangles made up of hyperphosphorylated tau protein. Beta-amyloid plaques disrupt synaptic communication between neurons, exerting neurotoxic effects, while tau tangles impair intracellular transport by obstructing the movement of essential molecules and nutrients within neurons. These pathological changes collectively contribute to synaptic dysfunction, neuronal degeneration, and ultimately widespread cognitive decline associated with Alzheimer's disease (4) Sah RP, et.al., (2024).

Although several pharmacological treatments are available for AD most of them provide only symptomatic relief and do not effectively stop or reverse the progression of neurodegeneration. In addition, their therapeutic benefits are often limited by variable effectiveness and the occurrence of undesirable side effects (5) Passeri E, et.al., (2022). These limitations have driven increasing interest in the use of plant based therapeutics as alternative or complementary strategies (6) Bhat BA, et.al., (2022). Medicinal plants, particularly those belonging to the *Araceae* family, are rich sources of diverse bioactive secondary metabolites such as flavonoids, triterpenoids, and phenolic compounds, which are known to exert multi-target neuroprotective effects. However, the complex nature of these multi-component systems makes it challenging to fully understand their mechanisms using conventional

experimental methods, thereby highlighting the need for integrated and systematic approaches to elucidate their precise actions within the central nervous system (7) Malik R, et.al., (2023).

In response to these challenges, the present study adopts an integrated approach combining in vitro and in silico techniques to investigate the therapeutic potential of *Colocasia esculenta*. Although this plant has been traditionally valued for its multifaced mechanism precise involvement in modulating pathways associated with Alzheimer's disease remains insufficiently explored, less undesirable effects, safe and easily available. Now, drug discovery is costlier affair, predict precision target and validate target efficacy with nominal cost, like using system biological disease protein and ligand interactions using artificial intelligence by computational and invitro studies, which are cost effective compared to various drug discovery studies for neuroprotective validation. By applying a multidisciplinary strategy like dry and wet lab, by system biology approach target, the study aims to elucidate the mechanisms underlying neuroprotection and to strengthen the scientific evidence supporting *Colocasia esculenta* as a potential therapeutic agent for Alzheimer's disease. (8) Zhang Z, et.al., (2024).

2. MATERIAL & METHODS

2.1 Plant Materials:

The plant material of *C. esculenta* (CE) was collected from Shahpur, Belgaum District, Karnataka, India, and its identity was verified by Dr. Harsha Hegde at the ICMR-National Institute of Traditional Medicine, Belagavi. A voucher specimen was deposited at the institute under the accession number RMRC-1960 for future reference.

2.2 Extraction of Plant Material:

The authenticated plant material of CE was washed thoroughly, cut into smaller pieces, and shade-dried at room temperature. The dried material was then pulverized into a coarse powder using a mechanical grinder. For extraction, 500 g of the powdered sample was macerated in 1500 mL of ethanol (1:3 w/v) with intermittent stirring for a duration of 7 days. Following maceration, the extract was filtered, and the solvent was evaporated at 40 °C to obtain a concentrated solid extract, which was preserved for subsequent studies (9) Widhyastini IGAM, et.al., (2018).

2.3 Preliminary Phytochemical Analysis:

The ethanolic extract of CE was analysed through preliminary qualitative phytochemical screening employing standard chemical assays to determine the presence of key phytochemical constituents, including carbohydrates, flavonoids, saponins, tannins, alkaloids, phenolic compounds and steroids (10) C.Ia U, et.al., (2025).

2.4 Estimation of Total Flavonoid Content:

The total flavonoid fraction of the CE extract was assessed using a modified aluminium chloride colorimetric method, with quercetin serving as the analytical standard. A stock solution of quercetin (100 µg/mL) was prepared by dissolving 10 mg of quercetin in 100 mL of 90% aqueous methanol, followed by serial dilutions to obtain concentrations ranging from 10 to 100 µg/mL. For the assay, 0.5 mL of each standard solution was combined with 1.5 mL of 90% aqueous methanol, 0.1 mL of 10% aluminium chloride, 0.1 mL of 1 M potassium acetate, and 2.8 mL of distilled water. The reaction mixture was incubated at room temperature for 30 minutes, after which absorbance was recorded at 415 nm using a UV-visible spectrophotometer. A blank solution was prepared by substituting aluminium chloride with distilled water. For sample estimation, 1 g of the extract was dissolved in 25 mL of 90% aqueous methanol and analysed using the same procedure. The flavonoid content was estimated using the quercetin standard curve and expressed in terms of quercetin equivalents (11) Sulastri E, et.al., (2018).

2.5 Estimation of Total Phenolic Content:

The total phenolic content of the CE extract was determined using the Folin-Ciocalteu method with slight modifications. Gallic acid was utilized to develop a standard calibration curve in the concentration range of 5–125 µg/mL. For the assay, 10 mg of extract was dissolved in 10 mL of methanol. A 0.5 mL aliquot of either standard or sample was mixed with 2.5 mL of 50% Folin-Ciocalteu reagent and 2.5 mL distilled water. After 5 minutes of incubation at room temperature, alkalization was achieved by adding 2 mL of 7.5% (w/v) sodium carbonate. After thorough shaking, the solution was incubated in darkness for 15 minutes. The absorbance was measured at a wavelength of 765 nm. In accordance with established protocols, the phenolic yield was calculated as gallic acid equivalents (µg GAE/mL) (11) Sulastri E, et.al., (2018).

2.6 In vitro Acetylcholinesterase Enzyme (AChE) Inhibitory Assay:

The inhibitory activity against acetylcholinesterase (AChE) was assessed utilizing the Ellman method (1961), beginning with the preparation of 1 mg/ml primary stock solutions for both the plant extract and the donepezil standard. These stocks were further diluted to establish a concentration gradient of 10, 20, 40, 80, 160 and 320 µg/ml for the extract and 1, 2, 4, 8, 16 and 32 µg/ml for donepezil. To execute the assay, 250 µl of each sample concentration was integrated into a reaction mixture containing 1.7 ml of 50 mM Tris-HCl buffer (pH 8.0), 10 µl of AChE enzyme (6.67 U/ml), and 20 µl of DTNB. Following a 15-minute incubation period, the enzymatic reaction was triggered by the addition of 10 µl of acetylthiocholine iodide. The subsequent kinetic changes were monitored spectrophotometrically at 412 nm, with absorbance readings recorded every 45 seconds for a 3-minute duration. By analysing the rate of absorbance change over time, the percentage of inhibition was determined, allowing for the calculation of the IC_{50} value through a correlation of inhibitory effects against the respective concentrations (12) Ellman GL, et.al., (1961).

3. COMPUTATIONAL PHARMACOLOGY

3.1 Mining of bioactive constituents and their information:

The bioactive compounds present in CE were compiled after an extensive review of scientific literature and consultation of several well-recognized phytochemical databases, such as Dr. Duke's Phytochemical and Ethnobotanical Databases (*http://phytochem.nal.usda.gov/*), and a long with other accessible public resources. This approach ensured that the list of constituents was comprehensive and supported by reliable data sources. Further chemical characterization of the identified compounds was carried out using information retrieved from PubChem (https://pubchem.ncbi.nlm.nih.gov/). From this database, key information including the molecular formula, molecular weight, and canonical SMILES (Simplified Molecular Input Line Entry System) notation was retrieved to facilitate further analysis.

3.2 Drug-likeness screening:

To assess whether the selected phytocompounds possess suitable pharmacokinetic properties, a drug-likeness evaluation was carried out using the Swiss ADME (https://www.swissadme.ch/) and MolSoft (https://www.molsoft.com/) online tools. Each compound was evaluated in accordance with Lipinski's Rule of Five, considering important parameters such as molecular weight, hydrogen bond donors and acceptors, lipophilicity (LogP), and the number of rotatable bonds. Compounds that satisfied these criteria were considered more likely to exhibit favourable drug-like behaviour and were therefore selected for subsequent target prediction studies.

3.3 Prediction of potential target proteins:

The probable biological targets of the selected phytocompounds were identified using publicly available databases such as SuperPred (https://prediction.charite.de/) and Swiss Target Prediction (https://www.swisstargetprediction.ch/). These platforms estimate potential targets by comparing the chemical structures of the compounds with known ligand-protein interactions. The predicted targets were then carefully checked and standardized using the UniProt (https://www.uniprot.org/) database to maintain uniformity and ensure accurate protein identification.

3.4 Identification of Scopolamine-induced disease targets:

Targets associated with scopolamine-induced memory impairment were collected from the Therapeutic Target Database (TTD) (https://ttd.idrblab.cn/) using relevant keywords such as scopolamine-induced cognitive impairment, memory deficit symptoms, and neurodegenerative disorders. Greater importance was given to targets with higher relevance scores to ensure their significance in the disease condition. The overlapping targets between the predicted protein targets of the selected phytocompounds and the disease-related proteins were subsequently identified using Venny diagram analysis with the Venny tool (https://bioinfogp.cnb.csic.es/tools/venny/). These common targets were considered as potential therapeutic targets for further analysis (13) Miravalles C, et.al., (2025).

3.5 Protein-protein interaction (PPI) network construction:

The overlapping targets were imported into the STRING database (https://string-db.org/) to analysed protein-protein interactions, with the interaction confidence score set to a high threshold to ensure reliability. The resulting PPI network was visualized and analysed using Cytoscape software 3.7.2 (https://cytoscape.org/release_notes_3_7_2.html). Topological characteristics of the network, including degree, betweenness centrality, closeness centrality, and edge connectivity, were analysed to determine hub proteins and critical regulatory nodes within the interaction network (14) Szklarczyk D, et.al., (2017).

3.6 Gene ontology and pathway enrichment analysis:

Functional enrichment analysis of the overlapping targets was performed using KEGG pathway and Gene Ontology (GO) databases via STRING. The enriched pathways related to metabolism, inflammation, oxidative stress, insulin resistance, and cardiovascular signalling were identified. Pathways with significant enrichment scores were selected to elucidate the mechanistic basis of clozapine-induced cardiometabolic toxicity and the protective potential of CE (15) Chen L, et.al., (2015).

3.7 Construction of compound-target-pathway network:

An integrated interaction network was constructed using Cytoscape software 3.7.2, incorporating phytoconstituent-target, target-pathway, and phytoconstituent-target-pathway interactions. Network topological analysis was performed using the edge count parameter to evaluate node connectivity. Nodes with higher edge counts were identified as key hubs, reflecting their central role and potential functional importance within the network (16) Shannon P, et.al., (2003).

3.8 Molecular Docking with Muscarinic Acetylcholine Receptor M1 (CHRM1) (PDB ID:5CXV) and Acetylcholinesterase (ACHE) (PDB ID: 7E3H)

Molecular docking was conducted to assess the binding affinity of candidate phytoconstituents against the CHRM1 (PDB ID: 5XCV) and ACHE (PDB ID: 7E3H) proteins, molecular docking simulations were performed. Ligand structures were obtained from the PubChem database and processed using Discovery Studio, while the active binding sites of both target proteins were predicted using the PrankWeb server. In silico docking was conducted using the PyRx AutoDock Vina platform, with a localized grid box centred over the predicted binding pocket for each target. Complexes exhibiting the lowest binding energy (kcal/mol) were prioritized for further study. Finally, post-docking analysis was performed in Discovery Studio to visualize and validate the stability of the molecular interactions, specifically focusing on hydrogen bonding and hydrophobic associations between the phytoconstituents and the receptor binding sites. (17) Kannan DrC. (2024).

3.9 Molecular dynamics Simulation:

Molecular dynamics simulations were employed to investigate the structural stability and binding dynamics of the CHRM1 (PDB ID: 5CXV) complex with pelargonidin-3-glucoside and the ACHE (PDB ID: 7E3H) complex with luteolin7-O-glucoside, molecular dynamics simulations were conducted utilizing the Desmond platform. For each system, the protein-ligand complex was immersed in a TIP4P solvent model within an orthorhombic simulation cell, with initial structural relaxation achieved through energy minimization using the OPLS4 force field to eliminate unfavourable contacts. Physiological ionic strength was replicated by adding sodium and chloride ions to a concentration of 0.15 M, The 100 nano seconds production runs were carried out under constant number of particles (N), pressure (P) and constant temperatures (T) NPT conditions, maintaining a temperature of 300 K and a pressure of 1.0132 bar, and trajectories were saved at 100 ps intervals, generating approximately 1,000 frames per simulation, which were subsequently evaluated via the Simulation Interaction Diagram module to determine key metrics, including backbone root mean square deviation (RMSD), residue-level root mean square fluctuation (RMSF), hydrogen bond persistence, and the overall stability of the interaction dynamics throughout the simulation period. (18) Ranade SD, et.al., (2024).

4.ANTIOXIDANT ASSAY

4.1 DPPH free radical scavenging activity:

The antioxidant activity of CE leaf extract was assessed using the DPPH free radical scavenging method. The extract was prepared using ethanol as the solvent and tested at different concentrations of 20, 40, 60, 80, and 100 µg/mL. Ascorbic acid was used as a standard reference compound for comparison. A freshly prepared 0.1 mM DPPH solution in ethanol was utilized for the assay, where 1 mL of the extract or standard were combined with 3 mL of the DPPH solution for each test. To ensure complete reaction, the samples were kept at room temperature for 30 minutes under dark conditions. Post-incubation, absorbance values were obtained at 517 nm via UV-Visible spectrophotometry. The resultant data were used to compute the percentage of antioxidant activity through the formula provided below:

$$\%\ Antioxidant\ activity = \frac{(Ac - At)}{Ac} \times 100$$

In the equation, Ac represents the control absorbance (DPPH solution without sample), while At denotes the absorbance measured for the test or standard solution (19) Baliyan S, et.al., (2022).

4.2 Ferric Ion-Reducing Antioxidant Power Assay (FRAP):

The ferric ion-reducing antioxidant capacity was determined using a modified procedure based on the method reported by Abbigeri M et al. Solutions of the extract and synthesized nanoparticles were prepared at concentrations ranging from 20 to 100 µg/mL. Each sample was mixed with 2.5 mL of 20 mM phosphate buffer (pH 6.6) and 2.5 mL of 1% potassium ferricyanide, followed by incubation at 50 °C for 30 minutes. After incubation, the reaction was terminated by adding 2.5 mL of trichloroacetic acid. Subsequently, 0.5% ferric chloride solution was added, and the mixture was allowed to stand for 10 minutes. The absorbance was then measured at 700 nm using

a UV-Visble spectrophotometer, with ascorbic acid serving as the standard reference. The reducing power was expressed as IC_{50} values, calculated from the concentration versus absorbance curve. Each experiment was carried out in triplicate to maintain accuracy and reproducibility of the findings. (20) Wojtunik-Kulesza KA. (2020) (21) Benzie IFF, et.al., (1996).

4.3 LC-MS analysis:

Metabolite profiling of the crude extracts was conducted via LC-MS using an Agilent 1260 Infinity II LC system coupled with an Agilent G6540B Q-ToF mass spectrometer operating in positive electrospray ionization (ESI+) mode. Distilled water extracts of dried leaf and samples were filtered through 0.25 µm polyvinylidene fluoride (PVDF) membrane syringe filters into 2 mL vials, followed by a 5 µL sample injection for chromatographic separation. Analytes were resolved on an Agilent Eclipse XDB-C18 column (150 × 3 mm, 3.5 µm) over a 30-minute run using a mobile phase consisting of (A) deionized water with 0.1% formic acid and (B) acetonitrile with 0.1% formic acid at a flow rate of 0.3 mL/min. The MS acquisition was set to a scan range of m/z 100 to 1700, with ion source parameters maintained at a nebulizer gas temperature of 300 °C, sheath gas temperature of 350 °C, drying gas flow of 8 L/min, sheath gas flow of 11 L/min, nebulizer pressure of 35 psig, capillary voltage of 3500 V, and nozzle voltage of 1000 V (22) Jagtap MA, et.al., (2025) (23) Mane MP, et.al., (2022).

5.RESULTS

5.1 Plant Extraction Yield:

The ethanolic extraction of CE produced a solid residue with a percentage yield of 9.8% (w/w), which was then utilized for subsequent experimental investigations.

5.2 Preliminary Phytochemical Screening:

Qualitative phytochemical screening of the ethanolic extract of CE. The leaves were found to contain essential primary metabolites like carbohydrates, along with a diverse range of bioactive secondary metabolites. The extract was found to contain alkaloids, flavonoids, tannins, phenolic compounds, saponins, and steroids. The occurrence of these phytoconstituents suggests that the extract possesses notable bioactive potential, supporting its relevance for further pharmacological exploration.

5.3 Total Flavonoid and Total Phenol:

The total flavonoid content of the extract was determined using the aluminium chloride colorimetric assay and quantified with reference to a quercetin standard calibration curve (Fig, 1A). The calibration exhibited excellent linearity, as indicated by the regression equation y = 0.0069x + 0.0078 with a correlation coefficient (R^2 = 0.9926), confirming the accuracy of the method. Based on this relationship, the flavonoid content, expressed as quercetin equivalents, was calculated to be 49.61 ± 3.41 µg/mL (Figure 1A). In a similar manner, the total phenolic content was evaluated using the Folin-Ciocalteu assay with gallic acid as the reference standard (Fig. 1B). The standard curve showed a strong linear correlation defined by the equation y = 0.004x + 0.0017 with an R^2 value of 0.9879, indicating good analytical precision. The phenolic content, expressed as gallic acid equivalents, was determined to be 73.74 ± 1.41 µg/mL. Overall, the results suggest that the extract is rich in phenolic and flavonoid constituents, which are likely responsible for its observed bioactive and antioxidant properties **(Figure 1)**.

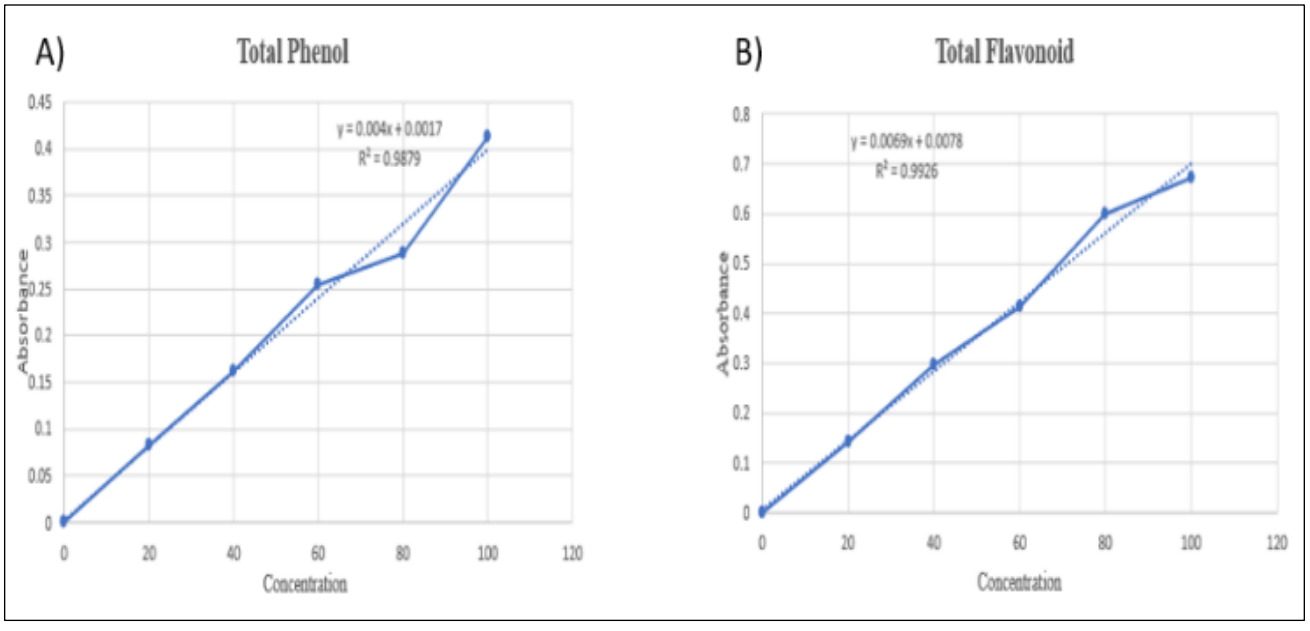

Figure 1: A) Total Flavonoid **B)** Total Phenol

5.4 In vitro ACHE Inhibitory Potential of CE:

The graph demonstrates the concentration-dependent inhibition of ACHE by CE extract and the reference standard donepezil. Both treatments exhibited a gradual increase in percentage inhibition with increasing concentration. CE showed inhibitory activity ranging from approximately 12.17% to 75.65% across the tested concentration range (10-320 µg/ml), whereas donepezil produced greater inhibition at lower concentrations, reaching approximately 71.30% at 8 µg/ml. These findings indicate that although donepezil displayed higher potency. CE also possessed significant ACHE inhibitory activity, suggesting its potential neuroprotective relevance in neurodegenerative disorders.

The IC50 of donepezil was found to be 3.61 µg/ml and the IC50 of CE extract was found to be 85.24 µg/ml. The ACHE inhibitory activity of donepezil was found to be more potent than that of CE **(Figure 2)**.

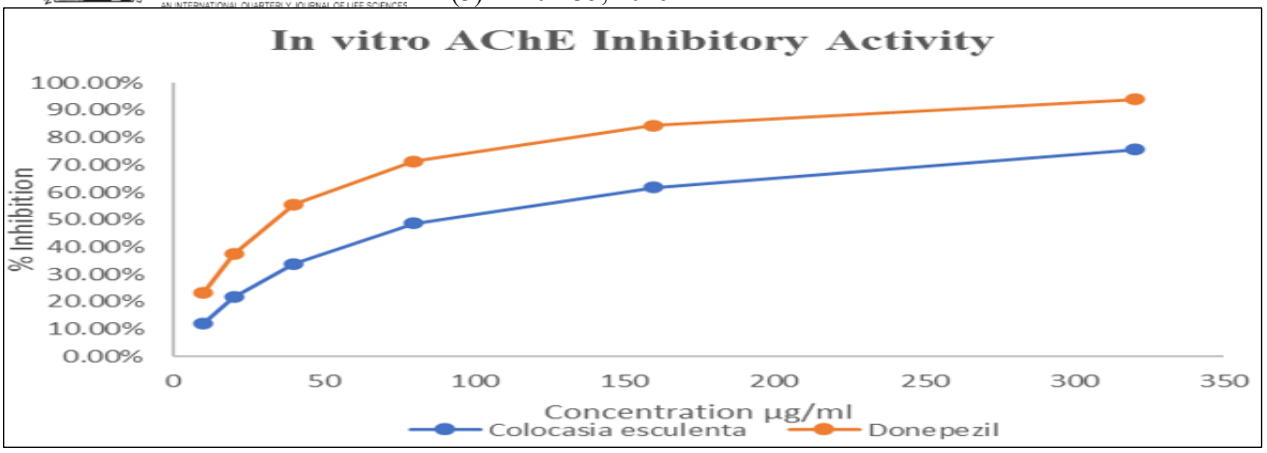

Figure 2: The graph demonstrates the concentration-dependent inhibition of AChE by CE extract and the reference standard donepezil. Both treatments exhibited a gradual increase in percentage inhibition with increasing concentration. CE showed inhibitory activity ranging from approximately 12.17% to 75.65% across the tested concentration range (10-320 µg/ml), whereas donepezil produced greater inhibition at lower concentrations, reaching approximately 71.30% at 8 µg/ml. These findings indicate that although donepezil displayed higher potency. CE also possessed significant AChE inhibitory activity, suggesting its potential neuroprotective relevance in neurodegenerative disorders.

5.5 Network Analysis:

The compound-target-pathway network of CE leaf phytoconstituents reveals a highly interconnected system underlying AD, comprising multiple nodes (bioactive compounds, protein targets, and pathways) linked through dense interactions that reflect a multi-target mode of action. Major pathways identified were PI3K-Akt, MAPK, cAMP, and calcium signaling, together with neuroactive ligand-receptor interaction and synaptic pathways (cholinergic, dopaminergic, and serotonergic), highlight disruptions in neuronal survival, synaptic plasticity, and neurotransmitter balance. Inflammatory and metabolic pathways such as IL-17 signalling, arachidonic acid metabolism, and gap junctions further indicate roles of neuroinflammation, oxidative stress, and impaired cellular communication in AD pathology. Network topology identified major hub targets, including CHRM1, GRIN1, GSK3B, DRD2 and ACHE, along with other key proteins such as GRIA2, MAOA, MAOB, PTGS2, HSP90AA1 and ADAM10, which are associated with cholinergic dysfunction, excitotoxicity, amyloid processing, and neuronal apoptosis. The interaction of multiple flavonoids and phenolic compounds with these targets supports a synergistic, multi-component therapeutic mechanism. Overall, the dense connectivity of the network suggests that CE exerts neuroprotective effects by modulating interconnected pathways involved in neurotransmission, inflammation, and neuronal survival, underscoring its potential in the management of AD **(Figure 3)**.

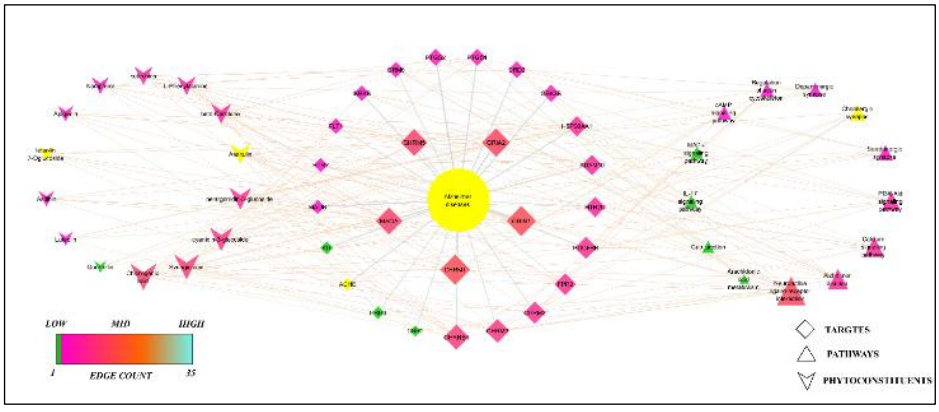

Figure 3: Network Analysis

5.6 Identification of Common Targets Using Venny Analysis:

A Venny diagram-based approach was employed to distinguish the overlapping as well as unique molecular targets between the predicted targets of CE and those linked to AD. The analysis demonstrated that a substantial proportion of targets, amounting to 762 (83.6%), were exclusively associated with CE (List 1). In contrast, 115 targets (12.6%) were identified as specific to AD (List 2). Notably, a smaller subset of 35 targets (3.8%) was found to be common to both groups, indicating potential key molecular points of interaction that may contribute to the therapeutic effects of CE in managing AD complications. The overall pattern of shared and distinct targets is represented in the Venny diagram **(Figure 4)**.

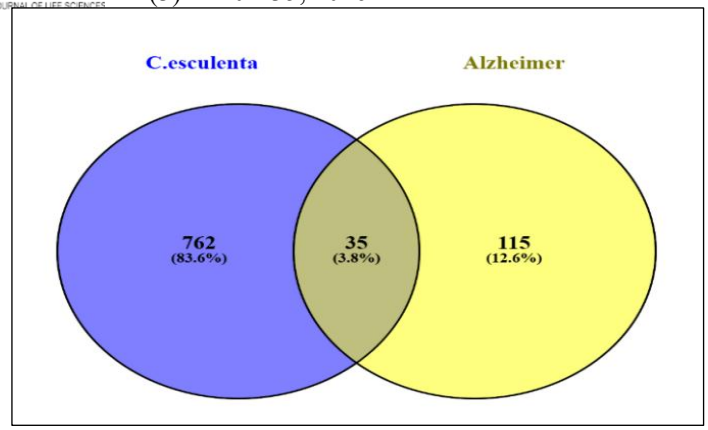

Figure 4: Common targets between CE and Alzheimer target

5.7 Gene ontology enrichment analysis:

The comprehensive Gene Ontology (GO) enrichment analysis spanning biological processes (BP), cellular components (CC), and molecular functions (MF) delineates a multifaceted mechanistic framework. At the biological process level, there was notable enrichment of terms associated with stimulus and chemical responses, including response to organic substance (GO:0010033), response to oxygen containing compound (GO:1901700), response to chemical (GO:0042221), and cellular response to chemical stimulus (GO:0070887) underscores that the involved genes such as CHRM1, GRM5, DRD2, GRIN1, MAO, PTGS2, and PRKCZ mediate adaptations to oxidative, metabolic, and neurotransmitter-related stress. These processes collectively reflect the network's capacity to regulate neuronal excitability, synaptic communication, and defence against neurotoxic injury processes that are central to maintaining neuronal integrity and cognitive function in Alzheimer's pathology. At the cellular component level, strong enrichment in membrane-associated and synaptic structures notably the plasma membrane (GO:0005886), postsynaptic membrane (GO:0045211), synaptic membrane (GO:0097060), dendrite (GO:0030425), and neuron projection (GO:0043005) highlights the localization of these proteins in neuronal membranes and synaptic compartments. These spatial associations emphasize roles in neurotransmission, receptor signalling, and ion channel regulation, all of which are critical for synaptic plasticity and neuronal signalling homeostasis. At the molecular function level, enrichment of neurotransmitter receptor and signalling terms such as neurotransmitter receptor activity (GO:0030594), G protein-coupled receptor activity (GO:0004930), acetylcholine receptor activity (GO:0015464), and protein kinase activity (GO:0004672) reveals that the identified targets participate in ligand-gated and GPCR-mediated neurotransmission, kinase signalling cascades, and receptor–ligand interactions that collectively sustain neuronal communication and adaptive responses to amyloid and oxidative stress. Altogether, these GO categories depict a coherent neuroprotective landscape in which neuronal membrane receptors, kinases, and synaptic proteins orchestrate signal transduction, neurotransmitter regulation, oxidative stress defence, and synaptic plasticity. This integrated functional architecture provides mechanistic insight into how multi-target modulation of signalling, receptor activity, and metabolic adaptation may collectively mitigate AD progression and associated neurodegeneration **(Figure 5)**.

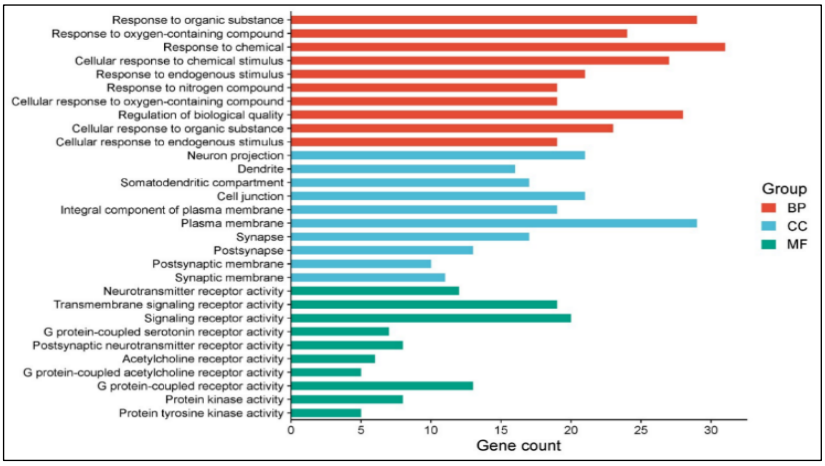

Figure 5: Gene ontology (GO) enrichment analysis

5.8 KEGG pathway analysis:

The KEGG pathway enrichment analysis reveals that neuroprotection against AD is governed by an integrated network of neurotrophic, calcium-regulated, inflammatory, and cell survival signalling pathways. Alzheimer's pathology characterized by amyloid-beta deposition, tau hyperphosphorylation, synaptic loss, and neuroinflammation is systematically addressed by the identified enriched pathways, centred on the AD pathway (hsa05010) where genes such as GSK3B, CASP3, LRRK2, and GRIN2B drive therapeutic modulation. This is complemented by the Calcium signalling pathway (hsa04020), involving GRIN2B, CHRM1, and CHRM3, which restores ionic homeostasis and prevents excitotoxicity to preserve synaptic plasticity. Vital to neuronal longevity, the PI3K-Akt signalling pathway (hsa04151) and Neuroactive ligand-receptor

interaction (hsa04080), featuring GSK3B, PIK3CB, and various HTR/DRD receptors, suppress pro-apoptotic signalling and maintain neurotransmitter balance, while the HIF-1 pathway (hsa04066) facilitates adaptation to cerebral oxidative stress through STAT3 and IKBKB. Metabolic flexibility is addressed through Insulin resistance (hsa04931) and Adipocytokine signalling (hsa04920), where PRKAA1 (AMPK) and SLC2A4 work to mitigate bioenergetic failure and Type 3 Diabetes phenotypes in the brain. Concurrently, inflammatory cascades such as TNF (hsa04668), IL-17 (hsa04657), and Toll-like receptor signalling (hsa04620) emphasize immune modulation, with regulation of PTGS2 (COX-2) and IKBKB attenuating microglial overactivation and cytokine-mediated neurodegeneration. Finally, the regulation of Apoptosis (hsa04210) and Necroptosis (hsa04217) via CASP3 and BAX limits irreversible neuronal loss and preserves the structural integrity of the hippocampus and cortex. Collectively, these pathways provide a comprehensive mechanistic framework illustrating how the coordinated regulation of calcium signalling, metabolism, inflammation, and cell survival underlies effective therapeutic strategies for AD **(Table1) (Figure 6)**.

Pathway ID	Term Description	Key Genes Involved
hsa05010	Alzheimer disease	*GSK3B, CASP3, LRRK2, GRIN2B*
hsa04020	Calcium signaling	*GRIN2B, CHRM1, CHRM3, PTGER3*
hsa04151	PI3K-Akt signaling	*GSK3B, PIK3CB, IKBKB, PTGS2*
hsa04668	TNF signaling	*PTGS2, IKBKB, CASP3*
hsa04066	HIF-1 signaling	*STAT3, IKBKB, PIK3CB*

Table 1: Key biological pathways with their term descriptions and genes involved

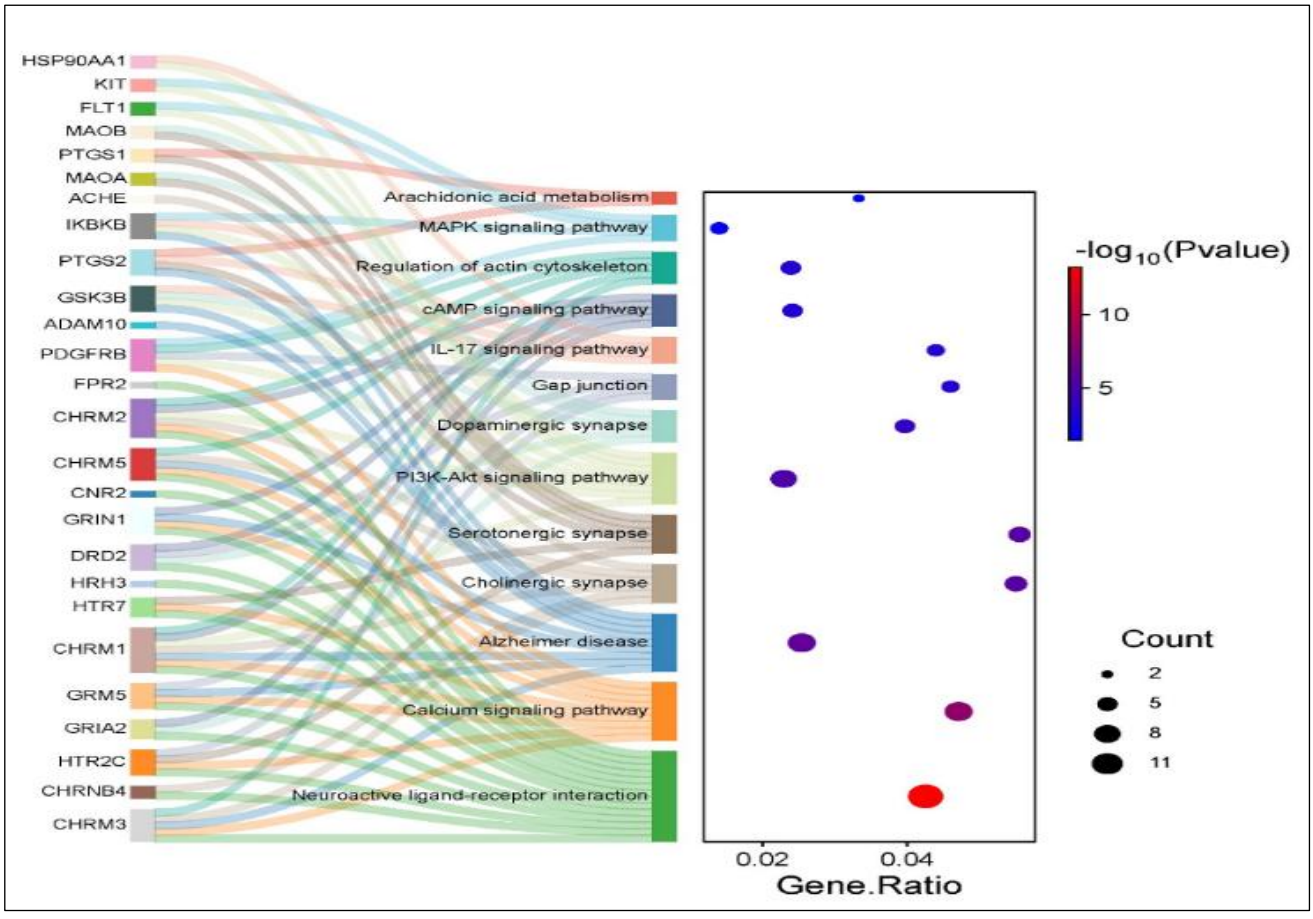

Figure 6: KEGG pathway analysis

5.9 Molecular Docking with Muscarinic Acetylcholine Receptor M1 (PDB ID: 5CXV)

Docking analysis was conducted to evaluate the interaction potential of the chosen compounds with the muscarinic acetylcholine receptor M1 (CHRM1; PDB ID: 5CXV). Among them, pelargonidin-3-glucoside demonstrated the highest binding affinity, achieving a docking score of -8.5. It was properly aligned within the active site and formed several conventional hydrogen bond interactions with key residues, including LEU183, ILE180, SER388, and TYR82, contributing to a stable complex formation. In addition, π-π stacking interactions were observed with aromatic residues such as TYR404 and TRP400, along with π-alkyl interactions involving VAL385, further enhancing the stabilization of the ligand within the active site. In comparison, cyanidin-3-glucoside displayed relatively lower binding affinity, with a docking score of -7.9. Although the compound was able to occupy the active site of

the receptor, the interaction profile suggested comparatively weaker binding stability. Overall, the docking findings suggest that pelargonidin-3-glucoside demonstrates stronger binding potential toward CHRM1 than cyanidin-3-glucoside, indicating its possible role as a promising modulator of the receptor **(Figure 7 and 8)**.

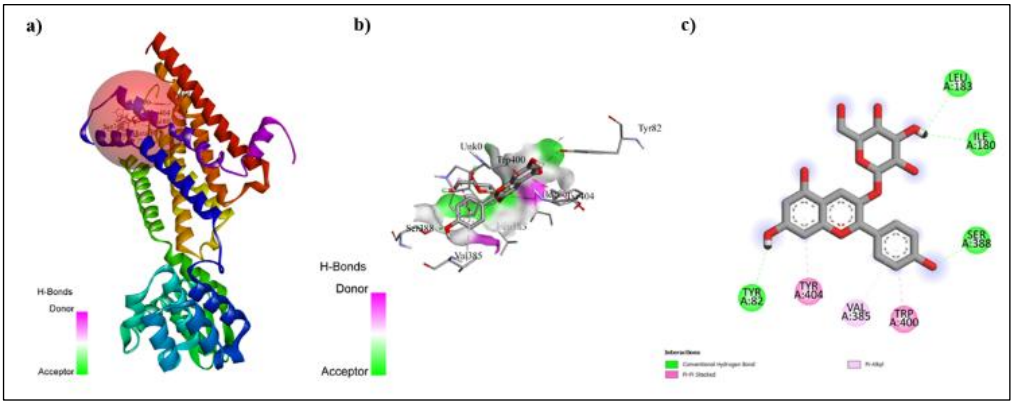

Figure 7: Intermolecular Interactions of pelargonidin-3-glucoside with CHRM1 (5CXV) (a) pelargonidin-3-glucoside at CHRM1 binding pocket; (b) 3D representation of pelargonidin-3-glucoside with CHRM1 at its residue site; (c) 2D representation of Ligand-Protein Contacts.

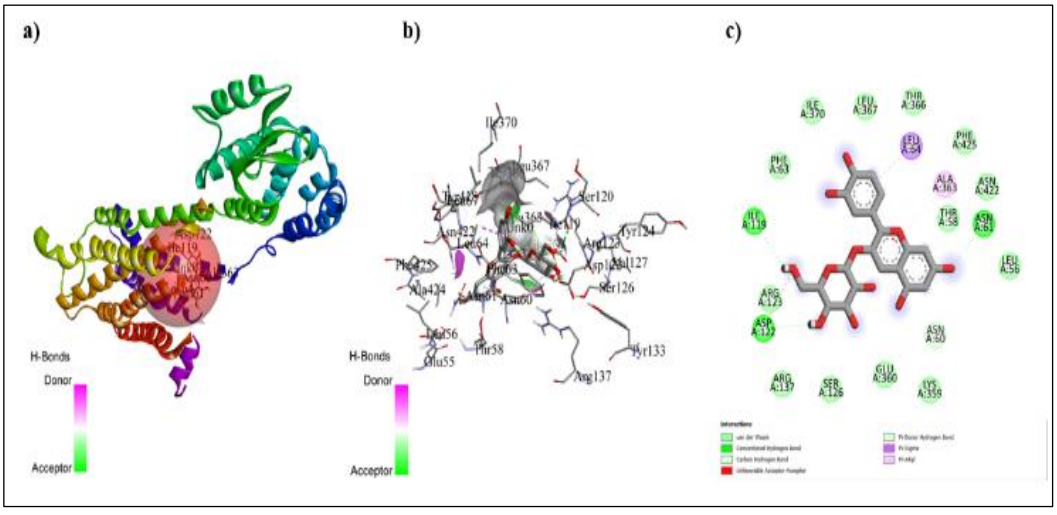

Figure 8: Intermolecular Interactions of cyanidin-3-glucoside with CHRM1 (5CXV) (a) cyanidin-3-glucoside at CHRM1 binding pocket; (b) 3D representation of cyanidin-3-glucoside with CHRM1 at its residue site; (c) 2D representation of Ligand-Protein Contacts.

5.10 Molecular Docking with Acetylcholinesterase (ACHE; PDB ID: 7E3H)

Molecular docking simulations were utilized to assess the binding affinity of selected phytoconstituents against the acetylcholinesterase (ACHE) enzyme, using PDB ID 7E3H as the target structure. The findings revealed that luteolin 7-O-glucoside achieved the highest binding potential with a docking score of -9.9 kcal/mol. This complex was stabilized within the active site through conventional hydrogen bond interactions with amino acid residues TYR103 and GLN322, alongside π-π stacking forces involving TRP317 and TYR372. Aesculin also exhibited significant binding strength, yielding a docking score of -9.7 kcal/mol, with its stability maintained by hydrogen bonds with GLU233 and TRP117 and a π-π T-shaped interaction with residue TYR372. Collectively, these data demonstrate that both compounds possess a high affinity for the ACHE enzyme, with luteolin 7-O-glucoside standing out as a particularly promising candidate for subsequent pharmacological development **(Figure 9 and 10)**.

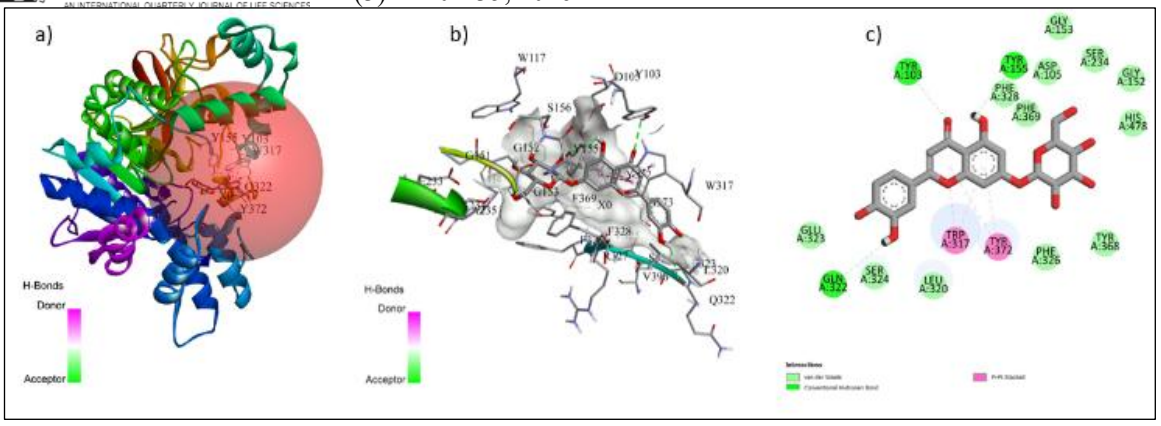

Figure 9: Intermolecular Interactions of luteolin 7-O-glucoside with ACHE (7E3H) (a) luteolin 7-O-glucoside at ACHE binding pocket; (b) 3D representation of luteolin 7-O-glucoside with ACHE at its residue site; (c) 2D representation of Ligand-Protein Contacts.

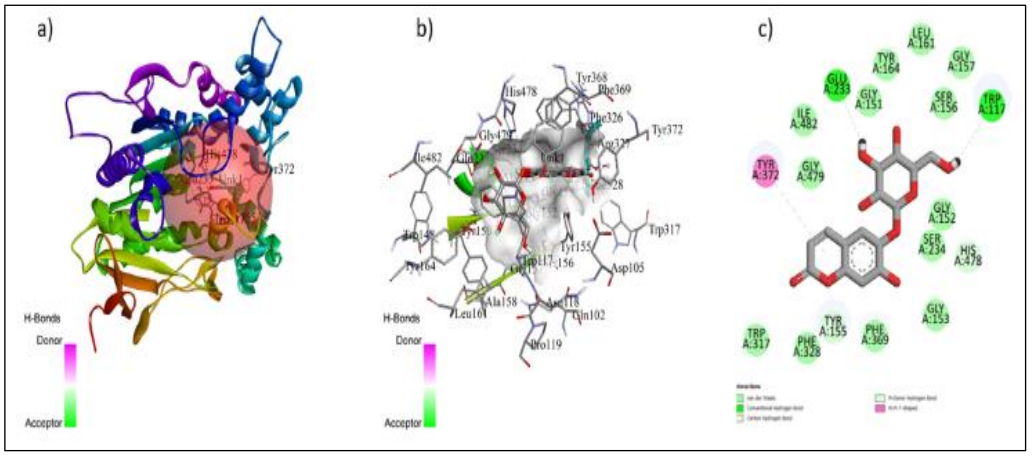

Figure 10: Intermolecular Interactions of aesculin with ACHE (7E3H) (a) aesculin at ACHE binding pocket; (b) 3D representation of aesculin with ACHE at its residue site; (c) 2D representation of Ligand-Protein Contacts.

5.11 Molecular dynamics Simulation of CHRM1 with pelargonidin-3-glucoside:

The molecular dynamics simulation of the CHRM1–pelargonidin-3-glucoside complex indicated consistent structural stability over the entire 100 ns trajectory. The protein exhibited RMSD values within the acceptable range of ~-3 Å for both Cα atoms and the backbone, indicating minimal structural deviation and proper equilibration without significant conformational drift. Ligand stability analysis showed that pelargonidin-3-glucoside maintained a consistent position within the binding pocket, with moderate RMSD variations relative to the protein, suggesting stable binding with minor conformational adjustments. RMSF profiling of the protein revealed localized flexibility primarily in loop and terminal regions, while core residues and secondary structural elements remained comparatively rigid. The ligand RMSF values indicated low atomic fluctuations when aligned to both the protein and itself, reflecting minimal internal flexibility and stable accommodation within the receptor binding site. Additionally, secondary structure analysis showed that approximately 67.41% of the protein maintained stable secondary structure elements, predominantly α-helices (64.41%), throughout the simulation. Protein–ligand interaction analysis further confirmed that the complex stability was supported by persistent hydrogen bonds, hydrophobic interactions, and water bridges over the simulation period. These findings collectively indicate that pelargonidin-3-glucoside forms a dynamically stable complex with CHRM1, maintaining consistent interactions while undergoing expected local fluctuations within the binding pocket **(Figure 11)**.

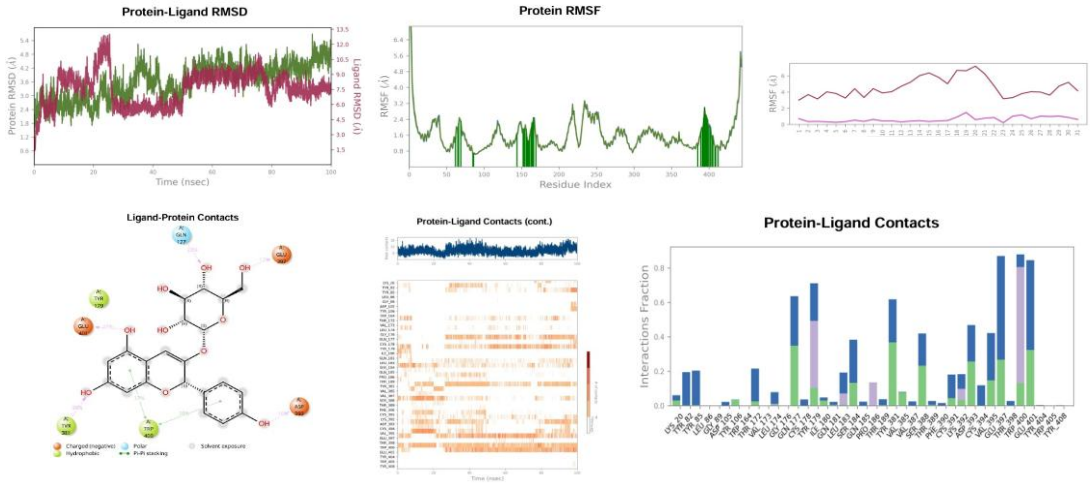

Figure 11: Molecular dynamics simulation of CHRM1 with pelargonidin-3-glucoside: a) Protein-ligand RMSD, b) Protein RMSD, c) Ligand RMSF d) Ligand-protein contacts, e) Protein-ligand contacts (cont.) f) Protein-ligand contacts

5.12 Molecular dynamics Simulation of ACHE with Luteolin7-O-glucoside:

The molecular dynamics simulation of the 7E3H-luteolin-7-O-glucoside complex revealed consistent structural stability throughout the 100 ns trajectory under NPT conditions at 310 K. The protein exhibited RMSD values within the acceptable range of approximately 1-3 Å for both Cα atoms and the backbone, indicating stable equilibration without significant conformational deviations. Ligand stability analysis revealed moderate RMSD fluctuations relative to the protein backbone, suggesting that luteolin-O-glucoside remained stably bound within the active site while undergoing minor conformational adjustments during the simulation. RMSF profiling of the protein indicated localized flexibility predominantly in loop and terminal regions, whereas the core residues and structured domains maintained lower fluctuation levels, reflecting structural rigidity. The ligand RMSF values showed limited atomic displacement when aligned to both the protein and itself, indicating minimal internal flexibility and stable accommodation within the binding pocket. Secondary structure analysis revealed that approximately 40.99% of the protein retained stable secondary structure elements, with α-helices contributing 28.51% and ß-strands 12.49% throughout the simulation, confirming the preservation of the overall fold. Furthermore, protein-ligand interaction analysis demonstrated that the complex was stabilized by persistent hydrogen bonds, hydrophobic contacts, ionic interactions, and water bridges maintained over a significant portion of the trajectory. These interactions collectively contributed to favorable binding and sustained ligand retention within the receptor binding site. Overall, the results indicate that luteolin-O-glucoside forms a dynamically stable complex with the 7E3H protein, maintaining consistent interactions while exhibiting expected localized fluctuations within the binding pocket **(Figure 12).**

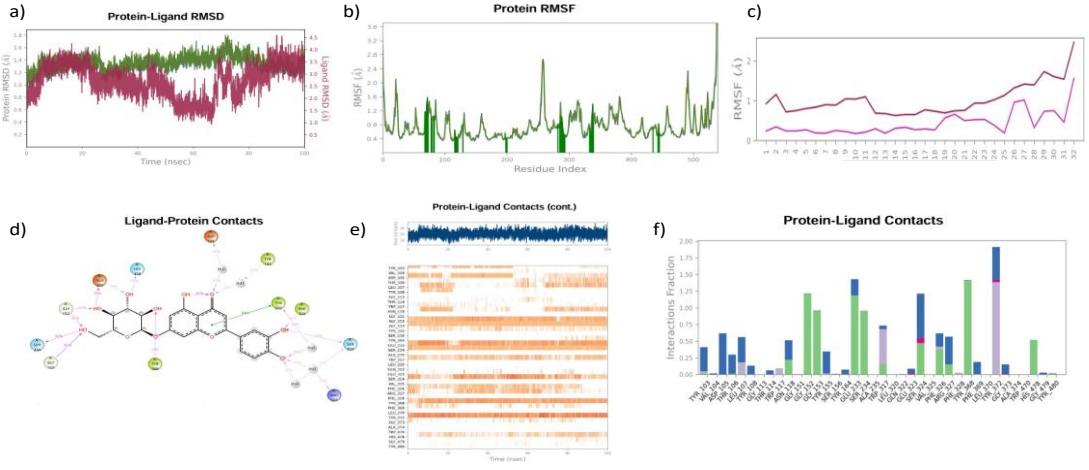

Figure 12: Molecular dynamics simulation of ACHE with luteolin 7-O-glucoside: a) Protein-ligand RMSD, b) Protein RMSD, c) Ligand RMSF d) Ligand-protein contacts, e) Protein-ligand contacts (cont.) f) Protein-ligand contacts.

5.13 DPPH Radical scavenging activity:

The antioxidant activity of the ethanolic leaf extract of *Colocasia esculenta* was evaluated using the DPPH radical scavenging assay, with an IC_{50} value of 51.49 µg/mL, indicating a moderately strong yet significant free radical scavenging activity. As depicted in the graph, the percentage inhibition increased progressively with increasing concentrations of the extract (20–100 µg/mL), demonstrating a clear dose-dependent response. Although the standard, ascorbic acid, exhibited higher antioxidant activity across

all concentrations, the extract consistently showed appreciable radical scavenging ability. This activity may be due to the presence of phytoconstituents that can donate hydrogen atoms or electrons potential natural source for mitigating oxidative stress **(Figure 13)**.

to neutralize DPPH radicals. Furthermore, the strong linear correlation (R^2 = 0.9985) supports the reliability of the observed trend. Overall, these findings suggest that *Colocasia esculenta* possesses notable antioxidant properties and may serve as a

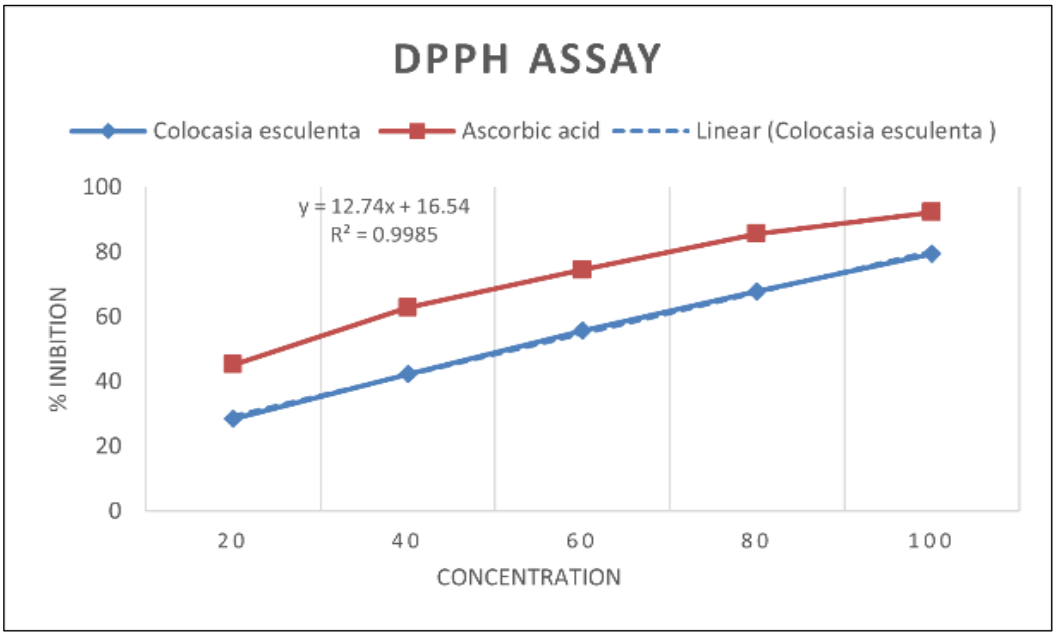

Figure 13: Free radical scavenging activity of Ascorbic acid and *Colocasia esculenta* extract. IC50 of ascorbic acid (25.45µg/mL) and IC50 of *Colocasia esculenta* extract was (51.49µg/mL)

5.14 FRAP ASSAY:

The IC_{50} value of the ethanolic leaf extract of *Colocasia esculenta* was calculated to be 47.55 µg/mL, suggesting a notable antioxidant capacity. The FRAP (Ferric Reducing Antioxidant Power) assay is based on the ability of antioxidant compounds to act as electron donors, facilitating the reduction of ferric ions (Fe^{3+}) to ferrous ions (Fe^{2+}). As depicted in the graph, the reducing activity of the extract increased steadily with rising concentrations, indicating a clear dose-dependent response in percentage scavenging activity.

Although the standard showed relatively higher reducing power, the extract exhibited a consistent and appreciable antioxidant effect throughout the tested range. This reducing ability can be attributed to the presence of phytoconstituents capable of neutralizing reactive oxygen species through electron donation. The transformation of ferricyanide (Fe^{3+}) to ferrocyanide (Fe^{2+}) further supports the strong reductive potential of the extract, highlighting its potential as a naturally occurring antioxidant source. Thus, the observed reducing power reflects the extract's effectiveness in counteracting oxidative stress and underscores its potential therapeutic significance **(Figure 14)**.

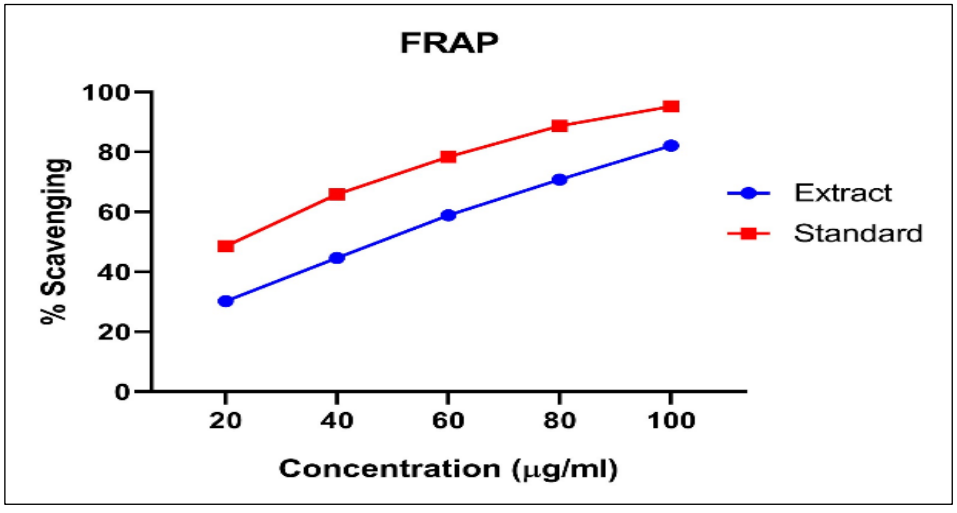

Figure 14: Dose-dependent FRAP Scavenging Effect of *Colocasia esculenta* Extract vs. Standard.

5.15 LCMS:

Liquid chromatography–mass spectrometry (LC–MS) analysis of the extract confirmed the presence of several bioactive phytoconstituents. The LC–MS spectra exhibited prominent molecular ion peaks corresponding to pelargonidin-3-glucoside (m/z 468.3097) and luteolin 7-O-glucoside (m/z 448.2192), as identified from their respective mass spectral profiles **(Figure 15)**.

A)

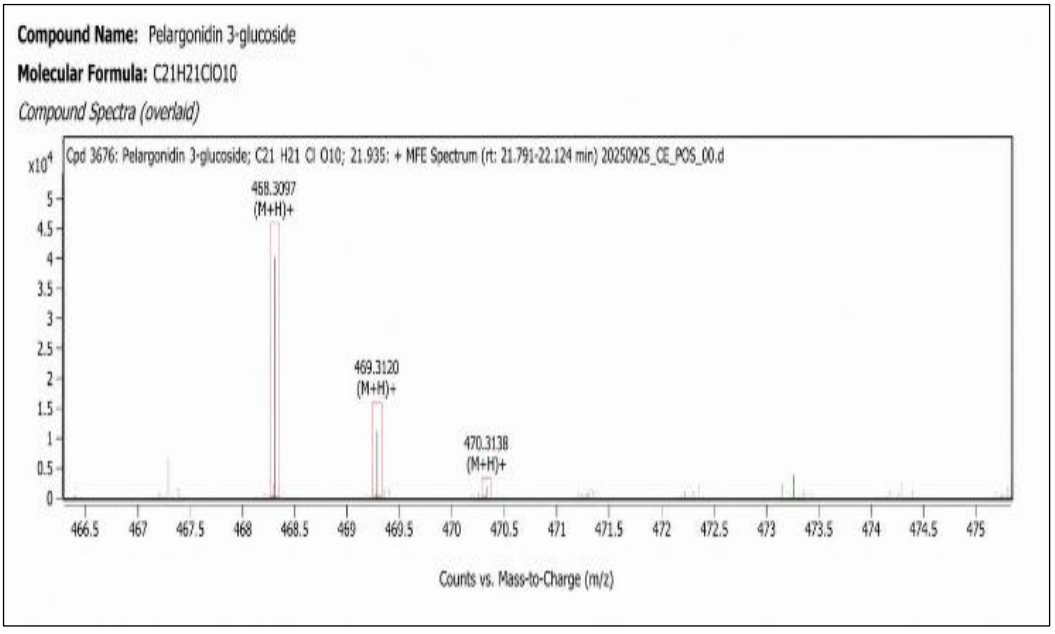

B)

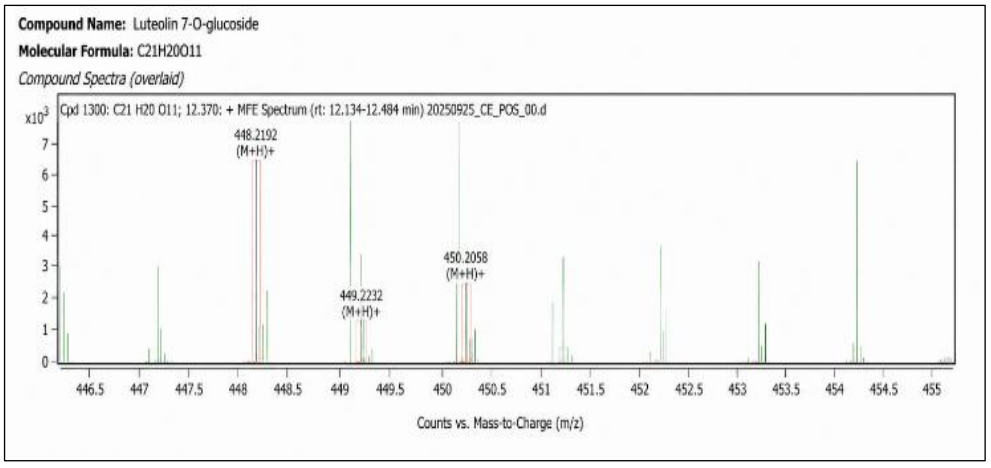

Figure 15: LC-MS analysis of *Colocasia esculenta* leaves extrac

6.DISCUSSION

Alzheimer's disease (AD) is a progressive neurodegenerative disorder associated with memory impairment, synaptic dysfunction, oxidative stress, cholinergic deficits, and chronic neuroinflammation. Although currently available therapeutic agents such as acetylcholinesterase inhibitors provide symptomatic improvement, they are unable to completely halt disease progression and are often associated with adverse effects during long-term use. Because of these limitations, increasing scientific attention has been directed toward medicinal plants containing multiple bioactive constituents capable of simultaneously targeting several pathological pathways involved in AD progression. In the present investigation, the neuroprotective potential of *Colocasia esculenta* was explored through a combination of phytochemical analysis, antioxidant evaluation, enzyme inhibition studies,

network pharmacology, molecular docking, and molecular dynamics simulation.

The phytochemical screening of the ethanolic extract revealed the presence of several secondary metabolites, including flavonoids, alkaloids, tannins, phenolic compounds, saponins, and steroids. Quantitative estimation further demonstrated high phenolic and flavonoid content, suggesting that the extract possesses substantial antioxidant potential. Earlier investigations on taro leaves and related medicinal plants have similarly demonstrated that phenolic-rich extracts exhibit strong free radical scavenging ability because phenolic hydroxyl groups can donate hydrogen atoms to neutralize reactive oxygen species. Previous studies involving flavonoid-containing plants have also shown that these compounds protect neuronal cells against oxidative damage and reduce neurodegeneration by suppressing lipid peroxidation and mitochondrial dysfunction. Therefore, the high phenolic and flavonoid content observed in the present study may significantly contribute to the neuroprotective activity of *C. esculenta*.

LC-MS profiling confirmed the presence of important flavonoid compounds such as pelargonidin-3-glucoside and luteolin 7-O-glucoside. These phytoconstituents have been previously reported to possess antioxidant, anti-inflammatory, and neuroprotective activities. Earlier experimental studies demonstrated that luteolin derivatives can inhibit the production of inflammatory mediators such as TNF-α, IL-6, and nitric oxide in activated microglial cells, thereby reducing neuronal inflammation associated with AD. Likewise, anthocyanin compounds such as pelargonidin derivatives were reported to improve neuronal survival and attenuate oxidative stress-induced apoptosis in experimental neurodegenerative models. Thus, the identification of these compounds in *C. esculenta* supports the possibility that the extract exerts therapeutic effects through multiple neuroprotective mechanisms.

Oxidative stress plays a major role in the initiation and progression of AD by promoting beta-amyloid aggregation, tau hyperphosphorylation, mitochondrial impairment, and neuronal apoptosis. In the current study, the extract demonstrated significant antioxidant activity in both DPPH and FRAP assays in a concentration-dependent manner. Similar antioxidant responses have been reported in several medicinal plants rich in flavonoids and polyphenols, where the extracts effectively scavenged free radicals and prevented oxidative neuronal damage. Previous experimental studies using neuroprotective plant extracts showed that reduction in oxidative stress was associated with improvement in memory and cognitive function in animal models of dementia. Therefore, the antioxidant activity observed in the present study may help in preventing oxidative neuronal injury associated with AD pathology.

Cholinergic dysfunction is considered one of the principal pathological features of AD because depletion of acetylcholine in the hippocampus and cerebral cortex contributes significantly to cognitive decline and memory impairment. In the present study, *C. esculenta* exhibited significant acetylcholinesterase inhibitory activity, although the potency was lower compared to donepezil. Earlier studies on flavonoid-rich medicinal plants demonstrated that natural compounds containing hydroxyl and glycosidic groups can bind effectively to the catalytic active site of acetylcholinesterase and inhibit its activity. Such inhibition prolongs the availability of acetylcholine within synaptic clefts and improves cholinergic neurotransmission. Previous investigations involving luteolin derivatives also demonstrated moderate to strong acetylcholinesterase inhibitory activity together with memory-enhancing effects in experimental cognitive dysfunction models. Therefore, the anti-cholinesterase activity observed in the present study suggests that *C. esculenta* may improve learning and memory functions by enhancing cholinergic signaling.

The network pharmacology analysis further demonstrated that the neuroprotective activity of *C. esculenta* involves a multi-target therapeutic mechanism. Multiple overlapping targets were identified between the phytoconstituents and AD-associated proteins, among which CHRM1, ACHE, GSK3B, DRD2, and GRIN1 were recognized as important hub proteins. Previous studies on AD pathogenesis have established that these proteins play major roles in neurotransmission, synaptic plasticity, amyloid processing, calcium homeostasis, and neuronal survival. Earlier network pharmacology investigations on herbal medicines used for neurodegenerative disorders similarly demonstrated that plant-derived compounds act through coordinated modulation of multiple interconnected signaling pathways rather than targeting a single receptor or enzyme. Such multi-target approaches are considered particularly beneficial in complex disorders like AD where multiple pathological mechanisms occur simultaneously.

Gene ontology and KEGG pathway enrichment analyses revealed significant involvement of pathways associated with PI3K-Akt signaling, calcium signaling, neuroactive ligand-receptor interaction, TNF signaling, IL-17 signaling, and inflammatory regulation. Previous experimental studies demonstrated that activation of the PI3K-Akt pathway suppresses apoptosis, improves neuronal survival, and inhibits tau hyperphosphorylation in AD models. Likewise, regulation of calcium signaling pathways has been shown to prevent excitotoxic neuronal injury caused by excessive glutamate receptor activation. Inflammatory pathways such as TNF and IL-17 signaling are strongly associated with microglial activation and chronic neuroinflammation in AD. Earlier reports demonstrated that suppression of these inflammatory mediators significantly reduced neuronal degeneration and cognitive impairment in experimental models. Therefore, the modulation of these pathways by *C. esculenta* suggests that the extract may exert broad neuroprotective effects through simultaneous regulation of oxidative stress, inflammation, and neuronal survival mechanisms.

Molecular docking analysis revealed strong interactions between the identified phytoconstituents and important AD-related targets. Luteolin 7-O-glucoside demonstrated high binding affinity toward acetylcholinesterase, while pelargonidin-3-glucoside exhibited favorable binding with CHRM1 receptors. Earlier molecular docking studies involving flavonoid compounds have similarly shown stable interactions with acetylcholinesterase and muscarinic receptors through hydrogen bonding, hydrophobic interactions, and π-π stacking interactions. These interactions are essential for stabilizing ligand binding within the active site and improving pharmacological activity. Previous studies investigating muscarinic receptor agonists also suggested that activation of CHRM1 receptors contributes to improved cognition, enhanced synaptic plasticity, and reduced amyloid toxicity in AD. Therefore, the docking observations in the present investigation strongly support the neuroprotective potential of the identified phytoconstituents.

The molecular dynamics simulation studies further validated the docking findings by confirming the structural stability of the ligand-protein complexes during the 100 ns simulation period. Stable RMSD and RMSF trajectories indicated that the ligands remained properly accommodated within the receptor binding pockets without significant conformational instability. Earlier molecular simulation studies reported that stable hydrogen bond interactions and minimal structural fluctuations are important indicators of sustained receptor-ligand interactions and long-term biological activity. Persistent hydrophobic interactions and water bridges observed during the present simulation further strengthened the stability of the complexes, suggesting that the identified phytoconstituents may effectively maintain receptor interactions under physiological conditions.

Overall, the present study demonstrates that *Colocasia esculenta* possesses considerable neuroprotective potential against Alzheimer's disease through antioxidant activity, acetylcholinesterase inhibition, anti-inflammatory effects, and modulation of multiple neuronal signaling pathways. Compared with previously published studies that primarily focused only on antioxidant or anti-inflammatory activities of medicinal plants, the current investigation provides a more comprehensive mechanistic understanding by integrating phytochemical characterization, network pharmacology, molecular docking, and molecular dynamics simulation. The findings collectively suggest that *C. esculenta* may serve as a promising multi-target therapeutic candidate for the management of Alzheimer's disease. However, further in vivo studies and clinical investigations are necessary to confirm its efficacy, safety, pharmacokinetic profile, and long-term therapeutic potential in neurodegenerative disorders.

7.CONCLUSION

This study investigated the neuroprotective potential of *Colocasia esculenta* (CE) against Alzheimer's disease (AD) using antioxidant FRAP assays and computational approaches. LC-MS analysis confirmed the presence of key bioactive compounds such as flavonoid including pelargonidin-3-glucoside and luteolin 7-O-glucoside. The extract exhibited significant anti-cholinesterase activity through effective inhibition of AChE, supporting restoration of cholinergic neurotransmission associated with memory and cognition. AChE and CHRM1 were identified as important molecular targets involved in acetylcholine regulation, neurogenesis, synaptic plasticity, and neuroinflammation. Molecular docking studies demonstrated strong binding affinities of luteolin 7-O-glucoside and pelargonidin-3-glucoside toward AChE and CHRM1, respectively. Additionally, 100 ns molecular dynamics simulations confirmed the structural stability of the protein–ligand complexes. Collectively, the findings suggest that *Colocasia esculenta* possesses promising multi-target neuroprotective activity against AD by reducing oxidative stress, synaptic dysfunction, and neuroinflammation while improving cognitive function and memory retention. Further preclinical animal studies and clinical investigations are necessary to validate the therapeutic efficacy and safety of the plant extract in Alzheimer's disease management.

8. REFERENCES

- Zhang XX, Tian Y, Wang ZT, Ma YH, Tan L, Yu JT. The Epidemiology of Alzheimer's Disease Modifiable Risk Factors and Prevention. J Prev Alzheimers Dis. 2021 Jul;8(3):313–21. doi:10.14283/jpad.2021.15
- Duan Y, Han C, Zheng H, Yu J, Luo M. Global, regional, and national burden of Alzheimer's disease and other dementias from 1990 to 2021: findings from the Global Burden of Disease Study 2021. Front Aging Neurosci. 2025 Dec 1;17:1678212. doi:10.3389/fnagi.2025.1678212
- Safiri S, Ghaffari Jolfayi A, Fazlollahi A, Morsali S, Sarkesh A, Daei Sorkhabi A, et al. Alzheimer's disease: a comprehensive review of epidemiology, risk factors, symptoms diagnosis, management, caregiving, advanced treatments and associated challenges. Front Med. 2024 Dec 16;11:1474043. doi:10.3389/fmed.2024.1474043
- Sah RP, Vidya C, Pereira P, Jayaram S, Yadav AK, Sujatha P. Neurotoxicity of Amyloid Beta and its Association with other Biomarkers in Pathogenesis of Alzheimer's Disease: A Narrative Review. J Clin Diagn Res. 2024. doi:10.7860/JCDR/2024/70332.20174
- Passeri E, Elkhoury K, Morsink M, Broersen K, Linder M, Tamayol A, et al. Alzheimer's Disease: Treatment Strategies and Their Limitations. Int J Mol Sci. 2022 Nov 12;23(22):13954. doi:10.3390/ijms232213954
- Bhat BA, Almilaibary A, Mir RA, Aljarallah BM, Mir WR, Ahmad F, et al. Natural Therapeutics in Aid of Treating Alzheimer's Disease: A Green Gateway Toward Ending Quest for Treating Neurological Disorders. Front Neurosci. 2022 May 16;16:884345. doi:10.3389/fnins.2022.884345
- Malik R, Kalra S, Pooja, Singh G, Meenu, Gahlot V, et al. Antioxidative and neuroprotective potential of Acorus calamus linn. and Cordia dichotoma G. Forst. In Alzheimer's type dementia in rodent. Brain Res. 2024 Jan;1822:148616. doi:10.1016/j.brainres.2023.148616
- Zhang Z, Cheng J, Zhou X, Wu H, Zhang B. Integrated network pharmacology and molecular docking to investigate the potential mechanism of Tufuling on Alzheimer's disease. Heliyon. 2024 Aug;10(16):e36471. doi:10.1016/j.heliyon.2024.e36471
- Widhyastini IGAM, Nurilmala F, Misja . Ethanol Extract (Colocasia esculenta (L.) Schott.) Hideung Cultivar as Anti-scabies through In-Vitro: In: Proceedings of the 1st International Conference on Recent Innovations [Internet]. Jakarta, Indonesia: SCITEPRESS - Science and Technology Publications; 2018 [cited 2026 Apr 1]. p. 2151–8. Available from: https://www.scitepress.org/DigitalLibrary/Link.aspx?doi=10.5220/0009940221512158 doi:10.5220/0009940221512158
- C.Ia U, S.Cb O, E.Jb N, C.Aa M, R.T S. Determination of Phytochemical Content of Dry Colocasia esculenta (cocoyam) Leaves Consumed by the People of Ezeagu in Enugu State, Nigeria. Int J Res Publ Rev. 2025 May;6(5):14919–14919. doi:10.55248/gengpi.6.0525.1964
- Sulastri E, Zubair MS, Anas NI, Abidin S, Hardani R, Yulianti R, et al. Total Phenolic, Total Flavonoid, Quercetin Content and Antioxidant Activity of Standardized Extract of Moringa oleifera Leaf from Regions with Different Elevation. Pharmacogn J. 2018 Nov 12;10(6s):s104–8. doi:10.5530/pj.2018.6s.20
- Ellman GL, Courtney KD, Andres V, Featherstone RM. A new and rapid colorimetric determination of

acetylcholinesterase activity. Biochem Pharmacol. 1961 Jul;7(2):88–95. doi:10.1016/0006-2952(61)90145-9

- Miravalles C, Cannon DM, Hallahan B. The effect of scopolamine on memory and attention: a systematic review and meta-analysis. Eur Psychiatry. 2025;68(1):e50. doi:10.1192/j.eurpsy.2025.2446
- Szklarczyk D, Morris JH, Cook H, Kuhn M, Wyder S, Simonovic M, et al. The STRING database in 2017: quality-controlled protein–protein association networks, made broadly accessible. Nucleic Acids Res. 2017 Jan 4;45(D1):D362–8. doi:10.1093/nar/gkw937
- Chen L, Chu C, Lu J, Kong X, Huang T, Cai YD. Gene Ontology and KEGG Pathway Enrichment Analysis of a Drug Target-Based Classification System. Wang J, editor. PLOS ONE. 2015 May 7;10(5):e0126492. doi:10.1371/journal.pone.0126492
- Shannon P, Markiel A, Ozier O, Baliga NS, Wang JT, Ramage D, et al. Cytoscape: A Software Environment for Integrated Models of Biomolecular Interaction Networks. Genome Res. 2003 Nov;13(11):2498–504. doi:10.1101/gr.1239303
- Kannan DrC. A Review on Step into the Future: Python Prescription (PyRx) Transforms Virtual Drug Discovery with AI-Driven Tools. Afr J Biomed Res. 2024 Sep 28;790–5. doi:10.53555/AJBR.v27i3S.2119
- 18 Ranade SD, Alegaon SG, Khatib NA, Gharge S, Kavalapure RS, Kumar BRP. Design, synthesis, molecular dynamic simulation, DFT analysis, computational pharmacology and decoding the antidiabetic molecular mechanism of sulphonamide-thiazolidin-4-one hybrids. J Mol Struct. 2024 Sep;1311:138359. doi:10.1016/j.molstruc.2024.138359
- Baliyan S, Mukherjee R, Priyadarshini A, Vibhuti A, Gupta A, Pandey RP, et al. Determination of Antioxidants by DPPH Radical Scavenging Activity and Quantitative Phytochemical Analysis of Ficus religiosa. Molecules. 2022 Feb 16;27(4):1326. doi:10.3390/molecules27041326
- Wojtunik-Kulesza KA. Approach to Optimization of FRAP Methodology for Studies Based on Selected Monoterpenes. Molecules. 2020 Nov 12;25(22):5267. doi:10.3390/molecules25225267
- Benzie IFF, Strain JJ. The Ferric Reducing Ability of Plasma (FRAP) as a Measure of "Antioxidant Power": The FRAP Assay. Anal Biochem. 1996 Jul;239(1):70–6. doi:10.1006/abio.1996.0292
- Jagtap MA, Magdum AB, Lugade VV, Kamble PS, Jayannawar DP, Nimbalkar MS, et al. Chemo-profiling by UPLC-QTOF-MS, GC-MS/MS analysis and in vitro bioactivity assessment of Desmodium gangeticum DC. South Afr J Bot. 2025 Oct;185:277–93. doi:10.1016/j.sajb.2025.07.047
- Mane MP, Patil RS, Magdum AB, Kakade SS, Patil DN, Nimbalkar MS. Chemo-profiling by UPLC-QTOF MS analysis and in vitro assessment of Anti-inflammatory activity of Field Milkwort (Polygala arvensis Willd.). South Afr J Bot. 2022 Sep;149:49–59. doi:10.1016/j.sajb.2022.05.043
- Zhang J, Zhang Y, Wang J, Xia Y, Zhang J, Chen L. Recent advances in Alzheimer's disease: mechanisms, clinical trials and new drug development strategies. Signal Transduct Target Ther. 2024 Aug 23;9(1):211. doi:10.1038/s41392-024-01911-3
- Shaikh JR, Patil M. Qualitative tests for preliminary phytochemical screening: An overview. Int J Chem Stud. 2020 Mar 1;8(2):603–8. doi:10.22271/chemi.2020.v8.i2i.8834
- Christou A, Parisis NA, Venianakis T, Barbouti A, Tzakos AG, Gerothanassis IP, et al. Ultrasound-Assisted Extraction of Taro Leaf Antioxidants Using Natural Deep Eutectic Solvents: An Eco-Friendly Strategy for the Valorization of Crop Residues. Antioxidants. 2023 Sep 26;12(10):1801. doi:10.3390/antiox12101801
- Galba Jean B, Alice Irène F, Albert Donatien A, Hervé-Hervé NA, Bertrand BM, Nanou Gael AD, et al. Neuroprotective Effects of the Ethanolic Leaf Extract of Crassocephalum crepidioides (Asteracaeae) on Diazepam-Induced Amnesia in Mice. Abdulah R, editor. Adv Pharmacol Pharm Sci. 2022 Sep 28;2022:1–10. doi:10.1155/2022/1919469
- Niwa Y, Kanda GN, Yamada RG, Shi S, Sunagawa GA, Ukai-Tadenuma M, et al. Muscarinic Acetylcholine Receptors Chrm1 and Chrm3 Are Essential for REM Sleep. Cell Rep. 2018 Aug;24(9):2231-2247.e7. doi:10.1016/j.celrep.2018.07.082
- Hopkins AL. Network pharmacology: the next paradigm in drug discovery. Nat Chem Biol. 2008 Nov;4(11):682–90. doi:10.1038/nchembio.118
- Li S, Zhang B. Traditional Chinese medicine network pharmacology: theory, methodology and application. Chin J Nat Med. 2013 Mar;11(2):110–20. doi:10.1016/S1875-5364(13)60037-0

- Hampel H, Hardy J, Blennow K, Chen C, Perry G, Kim SH, et al. The Amyloid-ß Pathway in Alzheimer's Disease. Mol Psychiatry. 2021 Oct;26(10):5481–503. doi:10.1038/s41380-021-01249-0
- Wang R, Reddy PH. Role of Glutamate and NMDA Receptors in Alzheimer's Disease. J Alzheimer's Dis. 2017 Apr 19;57(4):1041–8. doi:10.3233/JAD-160763
- Ashburner M, Ball CA, Blake JA, Botstein D, Butler H, Cherry JM, et al. Gene Ontology: tool for the unification of biology. Nat Genet. 2000 May;25(1):25–9. doi:10.1038/75556
- Razani E, Pourbagheri-Sigaroodi A, Safaroghli-Azar A, Zoghi A, Shanaki-Bavarsad M, Bashash D. The PI3K/Akt signaling axis in Alzheimer's disease: a valuable target to stimulate or suppress? Cell Stress Chaperones. 2021 Nov;26(6):871–87. doi:10.1007/s12192-021-01231-3
- Zhang Y, Lv S, Huang P, Xiao L, Lin N, Huang E. Network pharmacology study on the mechanism of berberine in Alzheimer's disease model. Npj Sci Food. 2025 Feb 4;9(1):16. doi:10.1038/s41538-025-00378-y
- Fisher A. Cholinergic Treatments with Emphasis on M1 Muscarinic Agonists as Potential Disease-Modifying Agents for Alzheimer's Disease. Neurotherapeutics. 2008 Jul;5(3):433–42. doi:10.1016/j.nurt.2008.05.002